

# Preferential Adsorption of Solvents on the Cathode Surface of Lithium Ion Batteries\*\*

Le Yu, Huijin Liu, Yan Wang, Naoaki Kuwata, Masatoshi Osawa, Junichi Kawamura, and Shen Ye\*

Lithium ion (Li-ion) batteries have replaced conventional batteries in most portable electronic devices, and are promising power source candidates for electric vehicles. This is mainly attributed to their high energy density and long cycle life.<sup>[1,2]</sup> Many new electrode materials for Li-ion batteries have been developed during the past decades to improve their energy density, charge/discharge rates, and service life.<sup>[3]</sup> Recently, more interest has focused on the surface states of the electrode/solution interface in Li-ion batteries, where the electrochemical reaction takes place to reduce the initial irreversibility and the capacity fading during cycling in which the electrolyte solutions play key roles.<sup>[4-6]</sup>

An ideal electrolyte solution for a Li-ion battery should have a high dielectric constant, low viscosity, high stability, and safety.<sup>[2,6]</sup> To meet these requirements, intensive studies have been devoted to the development of new types of electrolytes, such as ionic liquids and polymer electrolytes; however, carbonate esters are still the most widely used in today's commercial Li-ion batteries. Electrolyte solutions typically consist of cyclic carbonates, such as ethylene carbonate (EC) or propylene carbonates (PC), and linear carbonates, such as diethyl carbonate (DEC) or dimethyl carbonate (DMC), lithium salts, and various additives.<sup>[4]</sup> Although detailed results have been accumulated, the role of each component at the electrode surface (especially at the cathode surface) is still unclear. This significantly depends on our comprehensive understanding not only of the bulk properties of the electrolyte solutions, but also of their

structures on the electrode surface of Li-ion batteries on a molecular level. The latter remains a little-understood regime owing to the lack of surface-selective and sensitive in situ characterization techniques. For instance, XPS and NMR are powerful techniques to investigate the products on the electrode surfaces, but such analyses are possible only under ex situ conditions.<sup>[7,8]</sup> Vibrational spectroscopy techniques, such as IR and Raman spectroscopy, were employed to probe the structures in situ on the electrode/electrolyte interfaces of Li-ion batteries,<sup>[9-12]</sup> but these methods are intrinsically not surface-specific and usually not sensitive enough to study any formed monolayers.

Sum frequency generation (SFG) spectroscopy has been shown to be a powerful method for probing the molecular structures on various surfaces and interfaces owing to its high interface selectivity and sensitivity.<sup>[13-17]</sup> Recently, we reported an SFG study of the adlayer of PC solvent on the surface of  $\text{LiCoO}_2$ , which is the most widely used cathode material for Li-ion batteries, and revealed its unique adsorption geometries on the electrode surface.<sup>[18]</sup> Dlott and co-workers reported an SFG study of the adsorption of 1.0 M EC in tetrahydrofuran (THF) on gold and copper electrode surfaces.<sup>[19]</sup> These studies confirmed that SFG spectroscopy is a promising method to elucidate the solvent structures on the electrode surface of Li-ion batteries on a molecular level. It is expected that SFG measurements can be further employed to study the adsorption of solvents in Li-ion batteries with more practical electrolyte solutions. Herein, in situ SFG spectroscopy was employed to investigate the molecular structures at the  $\text{LiCoO}_2$  surface, contacting the electrolyte solutions of various pure and mixed carbonate ester solvents. Our results demonstrate that the structures and compositions of the solvent adlayers on the  $\text{LiCoO}_2$  surface are totally different from those of the bulk solutions and that EC is preferentially adsorbed on the  $\text{LiCoO}_2$  surface.

Figure 1a shows the *sps*-polarized SFG spectrum at the  $\text{LiCoO}_2$  surface contacting with EC/ $\text{LiClO}_4$  at the open circuit voltage (OCV; middle panel, circles) in the IR frequency region between 1700 and 1850  $\text{cm}^{-1}$ . The spectrum shows two strong bipolar bands, whereas nothing was observed at the  $\text{LiCoO}_2$ /air interface (spectrum not shown), indicating that the SFG signals are associated with the solvents. As SFG does not occur in a homogenous bulk solution with inversion symmetry, the present result suggests that the EC molecules align on the  $\text{LiCoO}_2$  surface with a certain ordered structure.

To quantitatively analyze the SFG spectra, SFG peak profiles ( $I_{\text{SFG}}$ ) were fitted with the following equation:

[\*] Dr. L. Yu, Dr. H. Liu, Y. Wang, Prof. M. Osawa, Prof. S. Ye  
Catalysis Research Center, Hokkaido University  
Sapporo 001-0021 (Japan)  
E-mail: ye@cat.hokudai.ac.jp  
Homepage: <http://www.cat.hokudai.ac.jp/osawa/member/ye>

Dr. N. Kuwata, Prof. J. Kawamura  
Institute of Multidisciplinary Research for Advanced Materials  
Tohoku University  
Sendai 980-8577 (Japan)

Dr. H. Liu  
Present address: Gannan Normal University (China)

[\*\*] Founding of this work is provided by the Li-EAD project of the New Energy and Industrial Technology Development Organization (NEDO). This work was also supported by a Grant-in-Aid for Scientific Research on Innovative Areas "Coordination Program" (24108701) and a Grant-in-Aid for Scientific Research (B) 23350058 from the Ministry of Education, Culture, Sports, Science & Technology (MEXT) (Japan). H.L. acknowledges a funding support (KJLD12089).

Supporting information for this article is available on the WWW under <http://dx.doi.org/10.1002/anie.201209976>.

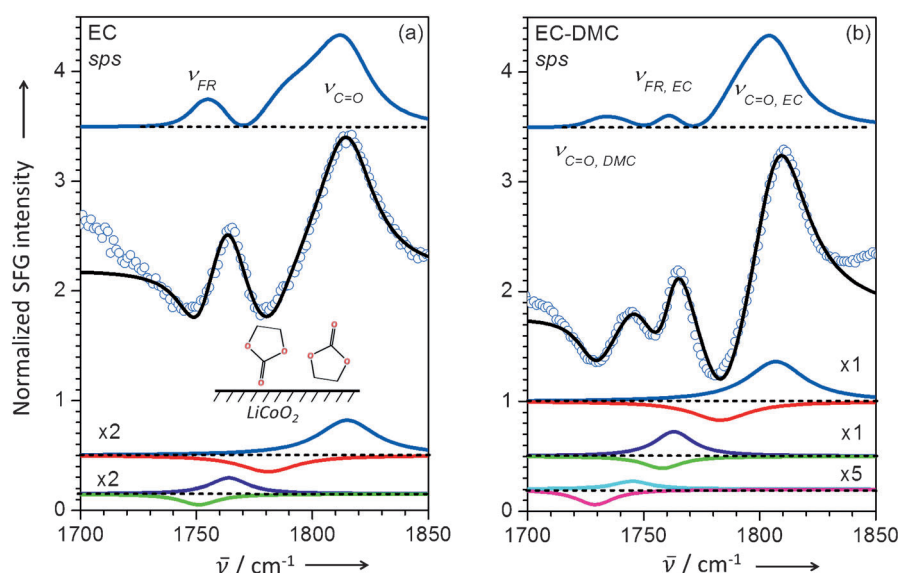


**Figure 1.** The *sps*-polarized SFG spectra of LiCoO<sub>2</sub> in contact with a) EC and b) EC + DMC (1:1 in volume) at the open-circuit voltage (OCV) in the IR region between 1700 and 1850 cm<sup>-1</sup>. Top panels: SFG spectra where  $\chi_{\text{NR}}^{(2)}$  are removed by fitting. Middle panels: SFG spectra (circle) and their fitting results (solid traces). Bottom panels: deconvoluted bands for the SFG spectra. The upward and downward peaks represent modes with reversed phases as the molecular model shown in inset. All of the spectra (except for the middle panels) are offset for clarity.

$$I_{\text{SFG}} \propto \left| \sum_{\nu} \frac{A_{\nu}}{\omega_{\text{IR}} - \omega_{\nu} + i\Gamma_{\nu}} e^{i\phi_{\nu}} + \chi_{\text{NR}}^{(2)} \right|^2 \quad (1)$$

where  $A_{\nu}$  and  $\Gamma_{\nu}$  are the amplitude and the damping constant, respectively, of the vibrational mode  $\nu$  at a frequency  $\omega_{\nu}$  with a phase angle ( $\phi_{\nu}$ ) with respect to the nonresonant signal ( $\chi_{\text{NR}}^{(2)}$ ). According to previous studies, two vibration modes of 1800–1820 and 1760–1770 cm<sup>-1</sup> are expected to be the vibrations of the EC molecules.<sup>[11,12,20–22]</sup> We were unable to obtain a decent fitting for the SFG spectrum by these modes assuming that all of the EC molecules take the same adsorption geometry on the LiCoO<sub>2</sub> surface; however, the observed SFG spectrum is well fitted under the assumption based on two adsorption geometries in reversed phase using Equation (1) (solid trace, middle panel, Figure 1a). Similar phenomena were also found for the adsorption of PC on the LiCoO<sub>2</sub> surface.<sup>[18]</sup> In this fitting, two pairs of vibration modes with four resonant components for the adsorbed EC are employed (bottom panel of Figure 1a). The vibrational pair at the higher frequency (1815 and 1780 cm<sup>-1</sup>, blue and red) are contributed by the C=O stretching mode ( $\nu_{\text{C=O}}$ ) of EC while the other pair in the lower frequency region (1765 and 1750 cm<sup>-1</sup>, purple and green) are assigned to the Fermi resonance ( $\nu_{\text{FR}}$ ) between the overtone between the ring breathing mode and C=O stretching mode.<sup>[11,12,20–23]</sup> Owing to the changes in the chemical environment, the vibrational modes in the same pair contributed by two adsorption geometries emerge at different frequencies and in reversed phases.

As shown in the inset of Figure 1a, because of the stronger interaction with LiCoO<sub>2</sub>, the strength of the C=O bond of the adsorbed EC pointing to the electrode is expected to be weaker than that pointing away from LiCoO<sub>2</sub>, result in a red-

shift from 1815 to 1780 cm<sup>-1</sup> and in reversed phases. Similarly, the peaks at 1765 and 1750 cm<sup>-1</sup> can be assigned to the  $\nu_{\text{FR}}$  mode of the adsorbed EC pointing its C=O group away and toward the electrode surface, respectively. As described in Equation (1), these modes optically interfere with  $\chi_{\text{NR}}^{(2)}$  as well as themselves, generating constructive (upward) and destructive (downward) peaks depending on the adsorption geometry of the molecules. The top panel in Figure 1a depicts the SFG spectrum after removing the nonresonant backgrounds by fitting, in which the bipolar-like peaks disappear, because the components only interfere with each other and not with  $\chi_{\text{NR}}^{(2)}$ . Based on the fitting results for the *sps*- and *ssp*-polarized SFG spectra for EC on the LiCoO<sub>2</sub> surface, the tilt angles of the C=O group of the two adsorption geometries for EC were estimated to be approximately  $12 \pm 2^{\circ}$  (1815 cm<sup>-1</sup>) and  $171 \pm 2^{\circ}$  (1780 cm<sup>-1</sup>) from the surface normal, respectively, in

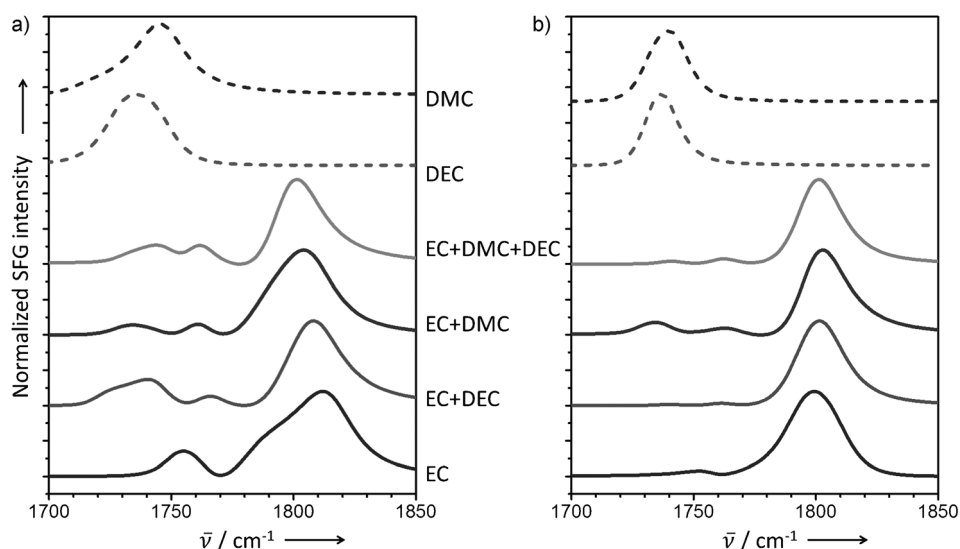
a molecular density ratio of 1.3 (see the Supporting Information), indicating that the carbonyl groups of the slightly more adsorbed EC molecules point toward the LiCoO<sub>2</sub> surface. On the other hand, as the overtone mode gains intensity at the expense of the fundamental vibration,<sup>[23]</sup> the  $\nu_{\text{FR}}$  modes were not used in the present calculation.

Figure 1b shows the SFG results for a binary mixed solvent of EC and DMC (middle panel, circles). The SFG spectrum of the mixed solvent looks similar to that of pure EC (Figure 1a) except for some weak contributions in the lower-frequency region. Along with the peaks from the adsorbed EC as mentioned above, an additional weak vibration pair around 1730 and 1745 cm<sup>-1</sup> is observed from fitting (Figure 1b, bottom panels). These peaks can be similarly attributed to the C=O stretching mode from DMC adsorbed on the electrode surface with different adsorption geometries.<sup>[10]</sup> Based on the fitting results for the binary mixture (solid trace, middle panel, Figure 1b), the molecular density of the adsorbed EC on the LiCoO<sub>2</sub> surface is almost 20 times higher than DMC, which is far from that in the bulk solution (see Table 1), indicating an intense enrichment of EC on the

**Table 1:** Molar percentages of EC in the bulk solution and on the LiCoO<sub>2</sub> surface in the mixed electrolyte solutions of the carbonate esters.

Composition, bulk [volume ratio]	EC in the bulk <sup>[a]</sup> [mol %]	EC on the surface <sup>[b]</sup> [mol %]
EC + DMC (1:1)	56	95
EC + DEC (1:1)	65	92
EC + DMC + DEC (1:1:1)	43	93

[a] Calculated from the liquid density. [b] Estimated from the present SFG measurements with error of  $\pm 1\%$ .



**Figure 2.** a) *sps*- and b) *ssp*-Polarized SFG spectra of the LiCoO<sub>2</sub> in contact with EC, EC + DEC, EC + DMC, EC + DMC + DEC, DEC, and DMC in the IR region between 1700 and 1850 cm<sup>-1</sup>. The nonresonant backgrounds were removed by fitting. The spectra were rescaled and offset for clarity.

LiCoO<sub>2</sub> surface. The top panel in Figure 1b shows the SFG spectrum of the EC + DMC mixed solution after removing  $\chi_{NR}^{(2)}$  by fitting, being very similar to that of EC.

The in situ SFG measurements were also carried out on LiCoO<sub>2</sub> contacting with other carbonate ester electrolyte solutions. Figure 2 summarizes the *sps*-polarized (a) and *ssp*-polarized SFG spectra (b) for the pure solvents of EC, DMC, DEC, and the binary mixtures of EC + DEC, EC + DMC, as well as the ternary mixture of EC + DMC + DEC after removing  $\chi_{NR}^{(2)}$  by fitting. Table 1 summarizes the analysis results based on SFG observations of the interface in various electrolyte solutions, and the molar ratios of EC in the bulk.

It is important to note that the spectral features of the mixed solvents of EC + DMC, EC + DEC, and EC + DMC + DEC solutions are dominated by EC in both the *sps*- and *ssp*-polarized SFG spectra. This indicates that the contribution to the SFG spectra from each component in the mixed solvents is significantly asymmetric, and is largely deviated from that in the bulk. For instance, the EC + DMC + DEC ternary mixed solution shows that the molar ratio of EC in the adlayer on the LiCoO<sub>2</sub> surface is 93 %, which is much higher than that in the bulk solution (43 %, Table 1). Similar results can also be found in the binary mixtures. These results strongly indicate the preferential adsorption of EC molecules on the LiCoO<sub>2</sub> surfaces compared to the linear carbonates, such as DEC and DMC.

To the best of our knowledge, this is the first direct evidence showing that the EC molecules are preferentially adsorbed on the LiCoO<sub>2</sub> surface from the electrolyte solutions of the mixed carbonate esters. This feature should be related to the extremely high dielectric constant of EC (89.8) in comparison with that of the linear carbonates of DEC (2.8) and DMC (3.1).<sup>[4]</sup> Thus, EC molecules are more easily polarized by an external field and the negatively charged C=O group of EC can strongly interact with the positively charged Li-ions. In fact, it has been confirmed by electrospray

ionization mass spectroscopy,<sup>[24,25]</sup> Raman<sup>[26]</sup> and NMR spectroscopy,<sup>[27]</sup> and theoretical calculations<sup>[28]</sup> that the Li-ions are preferentially solvated by the cyclic carbonates (such as EC) in the mixed electrolyte solutions than the linear carbonates (such as DMC and DEC). Considering that the effective concentration of Li-ions at the LiCoO<sub>2</sub> surface (> 20 mol L<sup>-1</sup>) is much higher than that in the electrolyte solution bulk, it is reasonable to assume that the binding strength between the LiCoO<sub>2</sub> surface and EC is much stronger than the nonpolar linear carbonates of DMC and DEC. The present observation agrees with the molecular dynamics (MD) calculation result for the EC + DMC solu-

tion on a graphite surface in which Vatamanu et al.<sup>[29]</sup> demonstrated that polar EC can replace DMC in the interfacial electrolyte layer when Li-ions are intercalated into graphite. Furthermore, the simulations based on the Monte Carlo method suggest that the EC dimer is thermodynamically stable owing to dipole–dipole interactions, which may stabilize the EC adlayer structure on the LiCoO<sub>2</sub> surface.<sup>[30]</sup>

On the other hand, IR reflection absorption spectroscopy observations of the solution on LiCoO<sub>2</sub> interface did not find such a preferential adsorption of EC.<sup>[11]</sup> This should be attributed to the low surface selectivity of the IR spectroscopy, especially for the adsorption of solvent, which is abundant in the bulk. In contrast to such a linear absorption spectroscopy, SFG collects information only from few layers of adsorbed molecules at the surface/interface. Therefore, it is worth noting that this is a significant advantage for SFG spectroscopy, which can quantitatively provide the structural information of the species only on the electrode surface.

In summary, we have successfully evaluated the adsorption structures of nonaqueous carbonate ester solvents including EC, DEC, DMC, and their binary and ternary mixtures, on the LiCoO<sub>2</sub> cathode surface on a molecular level by SFG vibrational spectroscopy and provided quantitative information about the adsorption and orientation of solvent molecules at the electrode/electrolyte interface in Li-ion batteries. Our study revealed that the preferential adsorption of the cyclic carbonate of EC molecules on the LiCoO<sub>2</sub> surface compared to the linear carbonates of DEC and DMC, with a largely different molecular proportion from that in the mixed solution bulk. These linear carbonates in the mixed electrolyte solutions play important roles in the bulk properties of the electrolyte solutions, such as the viscosity and melting point.

It should be noted that the present experiments were carried out on the LiCoO<sub>2</sub> cathode and electrolyte solution

interface at the OCV, just before the charging and discharging process starts. The present information will be useful to understand the initial stage for the solid electrolyte interphase (SEI) formation on the cathode surface. According to previous studies,<sup>[9,11–12,31]</sup> the surface states change significantly with the charging–discharging process, and the SFG measurements on LiCoO<sub>2</sub> cathode surface under potential control are in progress in our group. The fundamental understanding of the preferential adsorption of solvent under the potential control are expected to contribute both elucidation of the reaction mechanisms on the electrode surface of Li-ion batteries and development of novel solvents and additive materials for the purpose of improving the battery performance.

### Experimental Section

A LiCoO<sub>2</sub> thin film (ca. 50 nm thick) was deposited on the flat surface of a calcium fluoride (CaF<sub>2</sub>) prism by a pulsed laser deposition (PLD) method.<sup>[32]</sup> A broadband SFG system with a tunable femtosecond infrared pulse and a picosecond visible pulse was used for the in situ SFG measurements.<sup>[14,33–35]</sup> Polarization combinations are *sps* (that is, *s*-SFG/*p*-visible/*s*-IR) and *ssp*. SFG measurements were carried out at the LiCoO<sub>2</sub> surface in contact with different nonaqueous carbonate ester solutions containing LiClO<sub>4</sub> under the internal reflection mode. All the mixed solvents were prepared by mixing an equal volume of each component (Table 1). A temperature-controlled cell was designed for the in situ SFG observations. See the Supporting Information for details.

Received: December 13, 2013

Revised: February 28, 2013

Published online: April 24, 2013

**Keywords:** electrode–solution interfaces · lithium ion batteries · nonlinear vibrational spectroscopy · solvent adsorption

- [1] K. Mizushima, P. C. Jones, P. J. Wiseman, J. B. Goodenough, *Mater. Res. Bull.* **1980**, *15*, 783–789.
- [2] J. B. Goodenough, Y. Kim, *Chem. Mater.* **2010**, *22*, 587–603.
- [3] A. Manthiram, *J. Phys. Chem. Lett.* **2011**, *2*, 373–373.
- [4] K. Xu, *Chem. Rev.* **2004**, *104*, 4303–4417.
- [5] K. Xu, A. von Cresce, *J. Mater. Chem.* **2011**, *21*, 9849–9864.
- [6] V. Etacheri, R. Marom, R. Elazari, G. Salitra, D. Aurbach, *Energy Environ. Sci.* **2011**, *4*, 3243–3262.
- [7] D. Aurbach, B. Markovsky, A. Rodkin, E. Levi, Y. S. Cohen, H. J. Kim, M. Schmidt, *Electrochim. Acta* **2002**, *47*, 4291–4306.
- [8] N. Dupré, J. F. Martin, J. Oliveri, P. Soudan, A. Yamada, R. Kanno, D. Guyomard, *J. Power Sources* **2011**, *196*, 4791–4800.
- [9] T. Itoh, N. Anzue, M. Mohamedi, Y. Hisamitsu, M. Umeda, I. Uchida, *Electrochem. Commun.* **2000**, *2*, 743–748.
- [10] M. Moshkovich, M. Cojocaru, H. E. Gottlieb, D. Aurbach, *J. Electroanal. Chem.* **2001**, *497*, 84–96.
- [11] T. Matsushita, K. Dokko, K. Kanamura, *J. Power Sources* **2005**, *146*, 360–364.
- [12] M. Matsui, K. Dokko, K. Kanamura, *J. Power Sources* **2008**, *177*, 184–193.
- [13] P. B. Miranda, Y. R. Shen, *J. Phys. Chem. B* **1999**, *103*, 3292–3307.
- [14] J. Holman, P. B. Davies, T. Nishida, S. Ye, D. J. Neivandt, *J. Phys. Chem. B* **2005**, *109*, 18723–18732.
- [15] E. Tyrode, M. W. Rutland, C. D. Bain, *J. Am. Chem. Soc.* **2008**, *130*, 17434–17445.
- [16] S. Ye, M. Osawa, *Chem. Lett.* **2009**, *38*, 386–391.
- [17] S. Nihonyanagi, T. Ishiyama, T. Lee, S. Yamaguchi, M. Bonn, A. Morita, T. Tahara, *J. Am. Chem. Soc.* **2011**, *133*, 16875–16880.
- [18] H. Liu, Y. Tong, N. Kuwata, M. Osawa, J. Kawamura, S. Ye, *J. Phys. Chem. C* **2009**, *113*, 20531–20534.
- [19] P. Mukherjee, A. Lagutchev, D. D. Dlott, *J. Electrochem. Soc.* **2012**, *159*, A244–A252.
- [20] C. L. Angell, *Spectrochim. Acta* **1956**, *8*, 294.
- [21] B. Fortunato, P. Mirone, G. Fini, *Spectrochim. Acta Part A* **1971**, *27*, 1917–1927.
- [22] F. Joho, P. Novak, *Electrochim. Acta* **2000**, *45*, 3589–3599.
- [23] P. A. Brooksby, W. R. Fawcett, *Spectrochim. Acta Part A* **2001**, *57*, 1207–1221.
- [24] Y. Matsuda, T. Fukushima, H. Hashimoto, R. Arakawa, *J. Electrochem. Soc.* **2002**, *149*, A1045–A1048.
- [25] A. von Cresce, K. Xu, *Electrochem. Solid-State Lett.* **2011**, *14*, A154–A156.
- [26] S. K. Jeong, M. Inaba, Y. Iriyama, T. Abe, Z. Ogumi, *Electrochim. Acta* **2002**, *47*, 1975–1982.
- [27] V. P. Reddy, M. C. Smart, K. B. Chin, B. V. Ratnakumar, S. Surampudi, J. B. Hu, P. Yan, G. K. S. Prakash, *Electrochem. Solid-State Lett.* **2005**, *8*, A294–A298.
- [28] Y. X. Wang, P. B. Balbuena, *Int. J. Quantum Chem.* **2005**, *102*, 724–733.
- [29] J. Vatamanu, O. Borodin, G. D. Smith, *J. Phys. Chem. C* **2012**, *116*, 1114–1121.
- [30] L. B. Silva, L. C. G. Freitas, *J. Mol. Struct.* **2007**, *806*, 23–34.
- [31] D. Takamatsu, Y. Koyama, Y. Orikasa, S. Mori, T. Nakatsutsumi, T. Hirano, H. Tanida, H. Arai, Y. Uchimoto, Z. Ogumi, *Angew. Chem.* **2012**, *124*, 11765–11769; *Angew. Chem. Int. Ed.* **2012**, *51*, 11597–11601.
- [32] N. Kuwata, N. Iwagami, Y. Tanji, Y. Matsuda, J. Kawamura, *J. Electrochem. Soc.* **2010**, *157*, A521–A527.
- [33] S. Ye, H. Noda, S. Morita, K. Uosaki, M. Osawa, *Langmuir* **2003**, *19*, 2238–2242.
- [34] S. Ye, H. Noda, T. Nishida, S. Morita, M. Osawa, *Langmuir* **2004**, *20*, 357–365.
- [35] Y. Tong, Y. Zhao, N. Li, M. Osawa, P. B. Davies, S. Ye, *J. Chem. Phys.* **2010**, *133*, 034704.